2023 IEEE 97th Vehicular Technology Conference (VTC2023-Spring) | 979-8-3503-1114-3/23/$31.00 ©2023 IEEE | DOI: 10.1109/VTC2023-Spring57618.2023.10200984

Neural Network Based Node Prioritization for Efficient Localization

Carlos A. Gómez-Vega*, Moe Z. Win†, and Andrea Conti*

*Department of Engineering and CNIT, University of Ferrara, Via Saragat 1, 44122 Ferrara, Italy
(e-mail: cgomez@ieee.org, a.conti@ieee.org)

†Laboratory for Information and Decision Systems, Massachusetts Institute of Technology, Cambridge, MA 02139 USA
(e-mail: moewin@mit.edu)

***Abstract*—Optimizing the resource utilization is essential for efficiently providing reliable location awareness in complex wireless environments. This paper presents a data-driven approach to node prioritization for efficient localization based on neural networks. We develop a node prioritization strategy for power allocation consisting of offline training and online operation. In the offline phase, we train a neural network to approximate a mapping of node prioritization decisions obtained via model-based optimization. In the online phase, the trained neural network is employed to determine the resource allocation. A case study validates the proposed approach and compares it against conventional methods based on uniform power allocation.**

***Index Terms*—Localization, node prioritization, network operation, neural networks, optimization.**

I. Introduction

Location awareness [1] is crucial for numerous applications including autonomy [2], public safety [3], and the Internet-of-Things [4]. In location-aware networks, localization performance depends on the wireless resources, deployment of nodes, and propagation conditions. To achieve satisfactory performance, location-aware networks require efficient strategies for optimizing their operation [5]. Efficient network operation is challenging because the resource utilization must adapt to the wireless propagation conditions.

The Third Generation Partnership Project (3GPP) has defined positioning service level requirements in terms of accuracy, availability, and latency [6], [7]. Furthermore, energy efficiency is crucial to enable low-power high-accuracy localization and extend the network lifetime [8]. While localization algorithms have a key role in providing accurate localization [9], [10], network operation strategies are essential to obtain reliable position information and meet service-level requirements, especially in mission critical applications under resource constraints [11]. Network operation strategies for localization include allocation of wireless resources [12], selection and coordination of transmitting nodes [13], and placement of nodes [14]. In particular, node prioritization strategies for the allocation of wireless resources can benefit efficient localization by reducing the amount of transmissions and energy consumption.

Conventional network operation strategies focus on improving communication performance [15], [16]. Despite their effectiveness in providing reliable communication, their applicability for localization is restricted by the contrasting performance metrics in the design objectives. Specifically, node prioritization strategies for localization are developed in a model-based approach [12], [17], [18]. The design of such strategies involves establishing a system model and formulating an optimization problem. While such strategies can provide satisfactory gains in the localization performance, solving the underlying optimization problem can be prohibitive for reliable online operation. Furthermore, the parameter uncertainty can produce inadequate node prioritization decisions in complex wireless environments due to the use of simplified models. This motivates the use of data-driven approaches enabled by machine learning and, more specifically, neural networks.[1] In particular, data-driven solutions are considered to cope with the growing complexity of next generation networks [20].

The goal of this paper is to explore the use of neural networks to produce node prioritization decisions for efficient localization in a data-driven approach. The key idea is to exploit the approximation capabilities of neural networks [21] to fit a mapping of node prioritization decisions obtained via model-based optimization.

This paper presents a data-driven approach to node prioritization for efficient localization based on neural networks. We develop a two-phase node prioritization strategy consisting of offline training and online operation that exploits domain knowledge from model-based optimization. The key contributions of this paper are:

- development of a data-driven node prioritization strategy for efficient localization based on neural networks; and
- quantification of the localization performance gain provided by the proposed node prioritization strategy.

The remaining sections are organized as follows. Section II presents the system model and the node prioritization problem. Section III describes the proposed data-driven node prioritization strategy. Section IV presents a case study. Finally, Section V gives our conclusions.

Notations: Random variables are displayed in sans serif, upright fonts; their realizations in serif, italic fonts. Vectors and matrices are denoted by bold lowercase and uppercase letters, respectively. For example, a variable is denoted by x; a random vector and its realization are denoted by $\mathbf{x}$ and $\boldsymbol{x}$,

[1] Data-driven approaches based on machine learning have been explored recently for different applications in wireless communications [19].

respectively; a matrix is denoted by $\boldsymbol{X}$. Sets are denoted by calligraphic font. For example, a set is denoted by $\mathcal{X}$. The m-dimensional vector of zeros (resp. ones) is denoted by $\mathbf{0}_m$ (resp. $\mathbf{1}_m$): the subscript is removed when the dimension of the vector is clear from the context. The transpose of a vector $\boldsymbol{x}$ is denoted by $\boldsymbol{x}^{\mathrm{T}}$. The trace of a matrix $\boldsymbol{X}$ is denoted by $\mathrm{tr}\{\boldsymbol{X}\}$. The Euclidean norm and direction of a vector $\boldsymbol{x}$ are denoted by $\|\boldsymbol{x}\|$ and $\angle\boldsymbol{x}$, respectively. Notation $\boldsymbol{a} \succcurlyeq \boldsymbol{b}$ denotes that each element of vector $\boldsymbol{a}$ is greater than or equal to the corresponding element of vector $\boldsymbol{b}$.

II. Problem Formulation

This section describes the system model, presents the performance metric, and formulates the node prioritization problem.

A. System Model

Consider a 2D non-cooperative location-aware network composed by a single agent with unknown position and N_{b} anchors with known positions. We consider the single agent case because the localization processes of non-cooperative nodes are independent [22]. The index set of anchors is denoted by $\mathcal{N}_{\mathrm{b}} = \{1, 2, \ldots, N_{\mathrm{b}}\}$. The positions of the agent and anchor k are denoted by $\boldsymbol{p}$ and $\boldsymbol{p}_k$, respectively. The distance and angle between the positions of the agent and anchor k are denoted by $d_k(\boldsymbol{p}) = \|\boldsymbol{p} - \boldsymbol{p}_k\|$ and $\phi_k(\boldsymbol{p}) = \angle(\boldsymbol{p} - \boldsymbol{p}_k)$, respectively. The agent performs inter-node measurements with anchors to infer its position. The goal is to allocate the transmitting power for inter-node measurements to maximally improve localization performance. We consider that the total amount of available transmitting power is subject to a fixed upper constraint.

The received waveform for inter-node measurements between the agent and anchor k is modeled as

$$r_k(t) = \sqrt{u_k G} \sum_{l=0}^{L_k} \alpha_k^{(l)} s(t - \tau_k^{(l)}) + z_k(t) \tag{1}$$

where u_k is the transmitting power, G is a gain that depends on the antenna directivity and center frequency, $s(t)$ is the transmitted waveform, L_k is the number of received multipath components, $\alpha_k^{(l)}$ and $\tau_k^{(l)}$ are the amplitude and delay of the ray l, and $z_k(t)$ is the observation noise described by an additive white Gaussian process with two-sided power spectral density $N_0/2$. The coefficients of the wireless channel between the agent and anchor k are denoted by $\boldsymbol{w}_k = [\alpha_k^{(1)}, \tau_k^{(1)}, \alpha_k^{(2)}, \tau_k^{(2)}, \ldots, \alpha_k^{(L_k)}, \tau_k^{(L_k)}]^{\mathrm{T}}$.[2] The relationship between $\tau_k^{(l)}$ and the agent position is given by

$$\tau_k^{(l)} = \frac{1}{c}[d_k(\boldsymbol{p}) + b_k^{(l)}] \tag{2}$$

where c is the propagation speed of the signal and $b_k^{(l)} \geqslant 0$ is a range bias. More specifically, $b_k^{(1)} = 0$ and $b_k^{(1)} > 0$ for line-of-sight (LOS) and non-line-of-sight (NLOS) conditions, respectively [25].

[2]Note that $\boldsymbol{w}_k$ is a realization of the random vector $\mathbf{w}_k$ since the channel coefficients are described statistically (e.g., see [23], [24]).

B. Localization Performance Metric

The equivalent Fisher information matrix (EFIM) for the agent position $\boldsymbol{p}$ as a function of the node prioritization vector (NPV) $\boldsymbol{u} = [u_1, u_2, \ldots, u_{N_{\mathrm{b}}}]^{\mathrm{T}}$ can be expressed as [22]

$$\boldsymbol{J}(\boldsymbol{u}; \boldsymbol{p}, \boldsymbol{w}) = \sum_{k=1}^{N_{\mathrm{b}}} u_k \xi_k(\boldsymbol{p}, \boldsymbol{w}_k) \boldsymbol{J}_{\mathrm{r}}(\phi_k(\boldsymbol{p})) \tag{3}$$

where $\boldsymbol{w} = [\boldsymbol{w}_1^{\mathrm{T}}, \boldsymbol{w}_2^{\mathrm{T}}, \ldots, \boldsymbol{w}_{N_{\mathrm{b}}}^{\mathrm{T}}]^{\mathrm{T}}$. In particular, $\xi_k(\boldsymbol{p}, \boldsymbol{w}_k)$ is the range information intensity (RII) of the inter-node measurement with anchor k as a function of $\boldsymbol{p}$ and $\boldsymbol{w}_k$, and $\boldsymbol{J}_{\mathrm{r}}(\phi)$ is the range direction matrix (RDM) with angle ϕ. The RII $\xi_k(\boldsymbol{p}, \boldsymbol{w}_k)$ and RDM $\boldsymbol{J}_{\mathrm{r}}(\phi)$ are given, respectively, by

$$\xi_k(\boldsymbol{p}, \boldsymbol{w}_k) = \frac{8\pi^2\beta^2}{c^2}[1 - \chi_k(\boldsymbol{p}, \boldsymbol{w}_k)]\, \varrho_k(\boldsymbol{p}, \boldsymbol{w}_k) \tag{4a}$$

$$\boldsymbol{J}_{\mathrm{r}}(\phi) = \begin{bmatrix} \cos^2\phi & \cos\phi\sin\phi \\ \cos\phi\sin\phi & \sin^2\phi \end{bmatrix} \tag{4b}$$

where β is the effective bandwidth of the transmitted waveform $s(t)$, $\chi_k(\boldsymbol{p}, \boldsymbol{w}_k) \in [0, 1)$ is the path-overlap coefficient (POC) describing the degradation of the RII due to multipath propagation, and $\varrho_k(\boldsymbol{p}, \boldsymbol{w}_k) = G(\alpha_k^{(1)})^2/N_0$ is the signal-to-noise ratio (SNR) of the first received path.

The mean-square error of the position estimator as a function of the NPV $\boldsymbol{u}$ is lower bounded by

$$\mathcal{P}(\boldsymbol{u}; \boldsymbol{p}, \boldsymbol{w}) = \mathrm{tr}\Big\{\big[\boldsymbol{J}(\boldsymbol{u}; \boldsymbol{p}, \boldsymbol{w})\big]^{-1}\Big\} \tag{5}$$

which is referred to as the squared position error bound (SPEB) [22]. This performance metric can be employed for the design of node prioritization strategies since it is a measure of localization performance that is asymptotically achievable by maximum likelihood estimators [5].

C. Node Prioritization Problem

The node prioritization module aims to minimize the position error by optimally allocating the transmitting power for inter-node measurements with anchors. Specifically, the node prioritization problem can be formulated as

$$\mathscr{P}_{\boldsymbol{p},\boldsymbol{w}}: \ \underset{\boldsymbol{u}}{\text{minimize}} \quad \mathcal{P}(\boldsymbol{u}; \boldsymbol{p}, \boldsymbol{w}) \tag{6a}$$

$$\text{subject to} \quad \boldsymbol{u}^{\mathrm{T}}\mathbf{1} - P_{\mathrm{T}} \leqslant 0 \tag{6b}$$

$$\boldsymbol{u} \succcurlyeq \mathbf{0} \tag{6c}$$

in which (6b) describes the constraint on the total transmitting power P_{T} and (6c) indicates that the transmitting powers in the NPV are nonnegative.

The objective in (6a) is convex for $\boldsymbol{u} \succcurlyeq \mathbf{0}$ given $\boldsymbol{p}$ and $\boldsymbol{w}$ [5]. Therefore, $\mathscr{P}_{\boldsymbol{p},\boldsymbol{w}}$ is a convex program that can be solved via conventional convex optimization techniques, e.g., interior-point methods [26]. Such a problem can be further transformed into a second-order cone program (SOCP) to obtain a formulation that is more amenable to efficient optimization engines [5]. In particular, let $\boldsymbol{u}^* = [u_1^*, u_2^*, \ldots, u_{N_{\mathrm{b}}}^*]^{\mathrm{T}}$ denote the optimal solution to (6). The set of indices of the prioritized nodes in $\boldsymbol{u}^*$ is denoted by $\mathcal{N}_{\mathrm{p}}^* = \{k : u_k^* > 0\}$ with $N_{\mathrm{p}} = |\mathcal{N}_{\mathrm{p}}^*|$. The sparsity property of the optimal NPV [5] determines that the transmitting resources are allocated to at most three anchors, i.e., $N_{\rm p} \leqslant 3$. Such a property implies that only a subset of anchors will be used for inter-node measurements while keeping the rest inactive.

III. Data-driven Node Prioritization Strategy

This section describes the node prioritization strategy based on neural networks.

A. Node Prioritization Strategy

Node prioritization strategies based on (6) require knowledge of the agent position and channel coefficients for all the anchors in the network. In practice, such strategies rely on estimates of the agent position and channel qualities of a subset of anchors. In particular, solving (6) can be prohibitive for online operation due to the use of iterative optimization techniques, e.g., interior-point methods [26]. To address these issues, we consider a data-driven approach employing a neural network to fit a mapping of node prioritization decisions.

Consider that the agent performs measurements with a subset of $N_{\rm s}$ anchors in an arbitrary order to first obtain information regarding the channel qualities. From the sparsity property of the NPV, the node prioritization strategy requires knowledge from $N_{\rm s} \geqslant 3$ anchors. The set of indices of the anchors selected for such measurements is denoted by $\mathcal{N}_{\rm s} = \{s_1, s_2, \ldots, s_{N_{\rm s}}\} \subset \mathcal{N}_{\rm b}$. Such a subset can be any permutation of $\mathcal{N}_{\rm b}$ with cardinality $N_{\rm s}$. Note that the coefficients $\lambda_k = \xi_k(\boldsymbol{p}, \boldsymbol{w}_k)$ and $\varphi_k = \phi_k(\boldsymbol{p})$ summarize all the information regarding the wireless channel and network deployment with respect to anchor $k \in \mathcal{N}_{\rm b}$. Therefore, we rewrite the EFIM for the agent position $\boldsymbol{p}$ as a function of the NPV $\breve{\boldsymbol{u}} = [\breve{u}_1, \breve{u}_2, \ldots, \breve{u}_{N_{\rm s}}]^{\rm T}$ as

$$\breve{\boldsymbol{J}}(\breve{\boldsymbol{u}}; \boldsymbol{p}, \breve{\boldsymbol{\lambda}}, \breve{\boldsymbol{\varphi}}) = \sum_{k=1}^{N_{\rm s}} \breve{u}_k \breve{\lambda}_k \boldsymbol{J}_{\rm r}(\breve{\varphi}_k) \tag{7}$$

where $\breve{\boldsymbol{\lambda}} = [\breve{\lambda}_1, \breve{\lambda}_2, \ldots, \breve{\lambda}_{N_{\rm s}}]^{\rm T}$ and $\breve{\boldsymbol{\varphi}} = [\breve{\varphi}_1, \breve{\varphi}_2, \ldots, \breve{\varphi}_{N_{\rm s}}]^{\rm T}$ with $\breve{u}_k = u_{s_k}$, $\breve{\lambda}_k = \lambda_{s_k}$, and $\breve{\varphi}_k = \varphi_{s_k}$. With this parameterization, the SPEB can be rewritten as

$$\breve{\mathcal{P}}(\breve{\boldsymbol{u}}; \boldsymbol{p}, \breve{\boldsymbol{\lambda}}, \breve{\boldsymbol{\varphi}}) = \mathrm{tr}\Big\{ \big[\breve{\boldsymbol{J}}(\breve{\boldsymbol{u}}; \boldsymbol{p}, \breve{\boldsymbol{\lambda}}, \breve{\boldsymbol{\varphi}})\big]^{-1} \Big\}. \tag{8}$$

Then, we can reformulate the node prioritization problem as

$$\breve{\mathscr{P}}_{\boldsymbol{p}, \breve{\boldsymbol{\lambda}}, \breve{\boldsymbol{\varphi}}}: \ \underset{\breve{\boldsymbol{u}}}{\text{minimize}} \quad \breve{\mathcal{P}}(\breve{\boldsymbol{u}}; \boldsymbol{p}, \breve{\boldsymbol{\lambda}}, \breve{\boldsymbol{\varphi}}) \tag{9a}$$

$$\text{subject to} \quad \breve{\boldsymbol{u}}^{\rm T}\boldsymbol{1} - P_{\rm T} \leqslant 0 \tag{9b}$$

$$\breve{\boldsymbol{u}} \succcurlyeq \boldsymbol{0}. \tag{9c}$$

Note that the optimal solutions to problems (6) and (9) are equivalent if and only if $\mathcal{N}_{\rm p}^* \subset \mathcal{N}_{\rm s}$. In other words, the optimal solution to (9) provides the same performance obtained with the optimal solution to the problem with full knowledge of the channel coefficients and network deployment in (6) if the information of the anchors indexed by $\mathcal{N}_{\rm p}^*$ is available.

We consider an abstraction of the model-based optimization in (9) as a mapping of the node prioritization decisions, $\breve{\boldsymbol{u}}$, given the state $\boldsymbol{x} = [\boldsymbol{p}^{\rm T}, \breve{\boldsymbol{\lambda}}^{\rm T}, \breve{\boldsymbol{\varphi}}^{\rm T}]^{\rm T}$. Let $\mathcal{X}$ and $\mathcal{U}$ denote the state space and the decision space, respectively, such that $\boldsymbol{x} \in \mathcal{X}$ and $\breve{\boldsymbol{u}} \in \mathcal{U}$. The goal is to design a decision rule $f : \mathcal{X} \mapsto \mathcal{U}$. Let $\mathcal{F}$ denote a parametric family of decision rules with parameter space $\mathit{\Psi}$. For each $\boldsymbol{\psi} \in \mathit{\Psi}$, we have a decision rule $f(\boldsymbol{x}, \boldsymbol{\psi}) \in \mathcal{F}$. In particular, we develop a node prioritization strategy consisting of two phases, namely offline training and online operation. In the offline phase, we determine the parameters $\boldsymbol{\psi}$ that provide an adequate decision rule based on training data. Specifically, we consider a neural network architecture to approximate a mapping of the node prioritization decisions obtained by solving the model-based optimization in (6) [27]. In this regard, we exploit the approximation capabilities of fully-connected neural networks [21] to provide an abstraction of model-based optimization. In the online phase, the trained neural network is employed to determine the node prioritization decisions.

B. Offline Training

The goal of offline training is to determine the parameters $\boldsymbol{\psi} \in \mathit{\Psi}$ that provide an adequate mapping of node prioritization decisions based on training data. Let $\{\boldsymbol{y}^{(m)}, \boldsymbol{u}^{*(m)}\}_{m \in \mathcal{N}_{\rm train}}$ denote the training data indexed by $\mathcal{N}_{\rm train}$ considering the information from all the anchors in the network. In the generic case, $\boldsymbol{y} = [\boldsymbol{p}^{\rm T}, \boldsymbol{\lambda}^{\rm T}, \boldsymbol{\varphi}^{\rm T}]^{\rm T}$ is the state of the system with $\boldsymbol{\lambda} = [\lambda_1, \lambda_2, \ldots, \lambda_{N_{\rm b}}]^{\rm T}$ and $\boldsymbol{\varphi} = [\varphi_1, \varphi_2, \ldots, \varphi_{N_{\rm b}}]^{\rm T}$, and $\boldsymbol{u}^*$ is obtained by solving (6), e.g., by transforming the problem into an SOCP and using an interior-point method. We consider data augmentation [21] to take into account different subsets $\mathcal{N}_{\rm s}$ with arbitrary orders and the uncertainty of parameter estimation. For each instantiation of the augmented data, the subset $\mathcal{N}_{\rm s}$ includes the indices of the prioritized anchors and we consider estimates of $\boldsymbol{p}$, $\breve{\boldsymbol{\lambda}}$, and $\breve{\boldsymbol{\varphi}}$ while keeping the node prioritization decision $\breve{\boldsymbol{u}}$ fixed. Then, we have the augmented training data $\{\boldsymbol{x}^{(m)}, \breve{\boldsymbol{u}}^{*(m)}\}_{m \in \breve{\mathcal{N}}_{\rm train}}$ indexed by $\breve{\mathcal{N}}_{\rm train}$ with $|\breve{\mathcal{N}}_{\rm train}| > |\mathcal{N}_{\rm train}|$. Given a predefined neural network architecture, the goal is to determine the parameters $\boldsymbol{\psi}^* \in \mathit{\Psi}$ for its specific family of parametric decision rules $f(\boldsymbol{x}, \boldsymbol{\psi}) \in \mathcal{F}$ with $\boldsymbol{\psi} \in \mathit{\Psi}$. We refer the reader to [21] for details on training neural networks.

C. Online Operation

In the online phase, the location-aware network first obtains measurements from $N_{\rm s}$ anchors to retrieve the channel qualities. Given an estimate of the agent position, $\hat{\boldsymbol{p}}$, and estimates of the RIIs $\hat{\boldsymbol{\lambda}}$ and angles $\hat{\boldsymbol{\varphi}}$ with respect to the anchors with indices in $\mathcal{N}_{\rm s}$, the node prioritization module evaluates

$$\hat{\boldsymbol{u}} = f(\hat{\boldsymbol{x}}, \boldsymbol{\psi}^*) \tag{10}$$

where $\hat{\boldsymbol{x}} = [\hat{\boldsymbol{p}}^{\rm T}, \hat{\boldsymbol{\lambda}}^{\rm T}, \hat{\boldsymbol{\varphi}}^{\rm T}]^{\rm T}$. After evaluating (10), $\hat{\boldsymbol{u}}$ is post-processed to guarantee the fulfillment of the problem constraints, i.e., the total power constraint in (9b) and the nonnegativity of individual power levels in (9c). The post-processed NPV is the online node prioritization decision $\hat{\boldsymbol{u}}^*$.

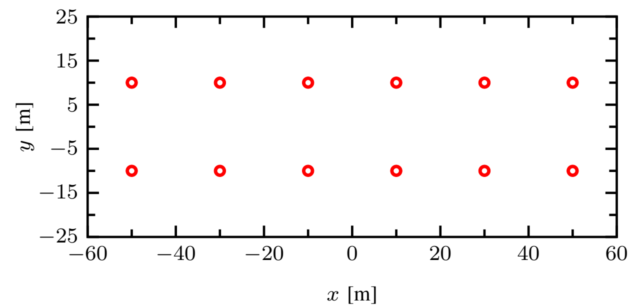

Fig. 1. Anchor deployment according to the 3GPP indoor open office layout.

IV. Case Study

This section validates the proposed node prioritization strategy in a case study. We consider ultra-wideband (UWB) technology [28] based on the IEEE 802.15.4a standard [29]. Specifically, $N_{\mathrm{b}} = 12$ anchors are placed according to the layout of the 3GPP indoor open office scenario (see Fig. 1) [23]. The nodes emit UWB root raised cosine pulses compliant with the IEEE 802.15.4a standard [29]. The channel coefficients are modeled according to the IEEE 802.15.4a channel model for the indoor office scenario [24]. We consider spatially-consistent LOS/NLOS states and channel coefficients [30] with the parameters of the 3GPP indoor open office scenario [23]. The RII between nodes in LOS conditions are determined following [31]. The RII between nodes in NLOS conditions is set to zero. The noise figure, center frequency, and maximum power spectral density are 10 dB, 6.489 GHz, and -41.3 dBm/MHz, respectively [29]. The transmitting power constraint is set to $P_{\mathrm{T}} = 200\,\mathrm{nW}$. The training dataset has $|\mathcal{N}_{\mathrm{train}}| = 10\,000$ instantiations of the node prioritization problem considering random placement of the agent and full knowledge of the scenario parameters. For each instantiation of training data, the node prioritization problem is solved using CVX [32]. The training data is augmented to $|\breve{\mathcal{N}}_{\mathrm{train}}| = 50\,000$ instantiations with the considerations in Section III-B. We consider 70% of the data for training and 30% for validation. The localization performance is evaluated on new instantiations of testing data.

We consider node prioritization strategies with $N_{\mathrm{s}} = 4, 5,$ and 6 anchors. For each value of N_{s} we train a different neural network architecture. We consider fully-connected neural networks consisting of three hidden layers with 64, 128, and 16 neurons, respectively. The input and output layers of each architecture have sizes of $2N_{\mathrm{s}} + 2$ and N_{s}, respectively. The activation functions are rectified linear units. We train the neural networks via backpropagation using the Adam algorithm [21] with 30 epochs and batch size of 128. The loss function for training is the half-mean-square error.

Table I shows the mean values of the root-mean-square error (RMSE) and loss function evaluated with training and validation data. The training and validation metrics are evaluated for the last batch in the training process and all the instantiations in the validation data, respectively. The small values of the RMSE and loss function indicate an adequate fitting of the desired mapping in the training phase. Note that the RMSE of the predicted NPV increases with N_{s}. For example, the values of the RMSE for 4 and 6 selected anchors are 0.40 and 0.58, which imply an increase of 45%. This increase is due to the sparsity in the optimal NPV since the trained neural network cannot predict exact zeros for the inactive nodes.

TABLE I
Training and validation results for different neural network architectures.

N_{s}	Training		Validation	
	RMSE	loss	RMSE	loss
4	0.40	0.08	0.47	0.11
5	0.48	0.12	0.57	0.16
6	0.58	0.17	0.64	0.20

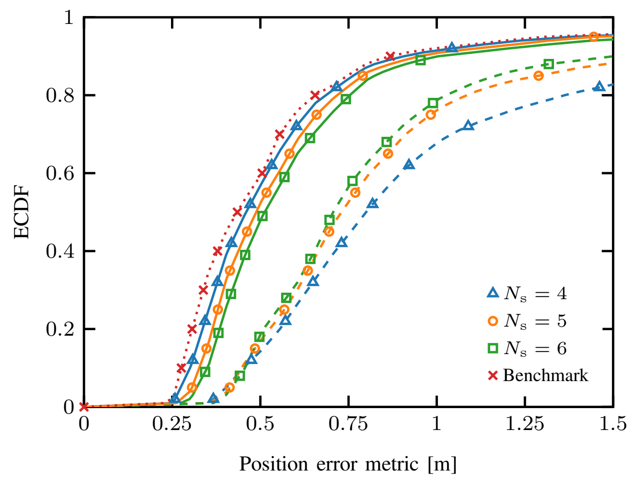

Fig. 2. ECDF of the position error metric for different node prioritization strategies based on random selection with uniform prioritization (dashed lines) and the proposed data-driven approach using neural networks (solid lines). The model-based optimization is shown as benchmark.

Next, we evaluate the performance provided by the trained neural network in online operation. We compare the following node prioritization strategies:

- model-based optimization — resource allocation based on (6) with full knowledge of the scenario parameters;
- random selection with uniform prioritization — N_{s} anchors in LOS conditions are selected randomly and the available power is equally divided among them;
- data-driven node prioritization — N_{s} anchors are selected and the resource allocation is performed with the trained neural network using estimated parameters.

In the latter strategy, we employ a second neural network for node selection based on the estimate of the agent position. The performance is evaluated in terms of the empirical cumulative distribution function (ECDF) of the position error metric (the square root of the SPEB).

Fig. 2 shows the performance of the proposed node prioritization strategies for different values of N_{s}. We can observe that the data-driven node prioritization strategies outperform conventional strategies based on random selection with uniform prioritization. In the latter strategies, increasing N_s improves the performance since it is more likely to select favorable nodes. In the data-driven node prioritization strategies, increasing N_s is not favorable due to a less accurate training (see Table I). Note that the performance of the data-driven node prioritization strategy with $N_\mathrm{s} = 4$ nodes approaches that of model-based optimization. For example, the position errors of the data-driven node prioritization strategy with $N_\mathrm{s} = 4$ and the model-based optimization at the 90th percentile are 0.91 and 0.87 m, respectively, implying a performance loss of 5%. At such mark, the strategy based on random selection with uniform prioritization for $N_\mathrm{s} = 6$ provides an error of 1.50 m. This implies that the data-driven strategy improves the performance by 42% with 2 active nodes less. While there is a slight loss compared to the benchmark, the proposed strategy based on neural networks is near-optimal with a reduced amount of information and under parameter uncertainty.

V. Conclusion

This paper presented a data-driven approach to node prioritization for efficient localization based on neural networks. We developed a node prioritization strategy for power allocation consisting of offline training and online operation that exploits domain knowledge from model-based optimization. Numerical results validate the proposed strategy and show its near-optimality with less information available and under parameter uncertainty. The domain knowledge incorporated in the offline phase enables efficient training of reliable node prioritization controllers. The proposed node prioritization strategy shows the effectiveness of neural networks for improving localization performance in complex wireless environments.

Acknowledgment

The fundamental research described in this paper was supported, in part, by the Office of Naval Research under Grant N62909-22-1-2009 and, in part, by the National Science Foundation under Grant CNS-2148251.

References

[1] M. Z. Win *et al.*, "Network localization and navigation via cooperation," *IEEE Commun. Mag.*, vol. 49, no. 5, pp. 56–62, May 2011.

[2] A. Guerra, F. Guidi, D. Dardari, and P. M. Djurić, "Networks of UAVs of low complexity for time-critical localization," *IEEE Aerosp. Electron. Syst. Mag.*, vol. 37, no. 10, pp. 22–38, Oct. 2022.

[3] A. R. Ansari, N. Saeed, M. I. Ul Haq, and S. Cho, "Accurate 3D localization method for public safety applications in vehicular ad-hoc networks," *IEEE Access*, vol. 6, pp. 20 756–20 763, 2018.

[4] L. Chen *et al.*, "Robustness, security and privacy in location-based services for future IoT: A survey," *IEEE Access*, vol. 5, pp. 8956–8977, Apr. 2017.

[5] M. Z. Win, W. Dai, Y. Shen, G. Chrisikos, and H. V. Poor, "Network operation strategies for efficient localization and navigation," *Proc. IEEE*, vol. 106, no. 7, pp. 1224–1254, Jul. 2018.

[6] *Technical Specification Group Services and System Aspects; Service requirements for the 5G system; Stage 1*, 3rd Generation Partnership Project 3GPP™ TS 22.261 V18.6.0 (2022-03), Mar. 2022, Release 18.

[7] A. Conti *et al.*, "Location awareness in beyond 5G networks," *IEEE Commun. Mag.*, vol. 59, no. 11, pp. 22–27, Nov. 2021.

[8] *Technical Specification Group Services and System Aspects; Service requirements for cyber-physical control applications in vertical domains; Stage 1*, 3rd Generation Partnership Project 3GPP™ TS 22.104 V18.3.0 (2021-12), Dec. 2021, Release 18.

[9] X. Wang, X. Wang, and S. Mao, "Deep convolutional neural networks for indoor localization with CSI images," *IEEE Trans. Netw. Sci. Eng.*, vol. 7, no. 1, pp. 316–327, Jan.-Mar. 2020.

[10] A. Conti, S. Mazuelas, S. Bartoletti, W. C. Lindsey, and M. Z. Win, "Soft information for localization-of-things," *Proc. IEEE*, vol. 107, no. 11, pp. 2240–2264, Nov. 2019.

[11] *Technical Specification Group Services and System Aspects; Mission Critical Services Common Requirements (MCCoRe); Stage 1*, 3rd Generation Partnership Project 3GPP™ TS 22.280 V19.0.0 (2022-12), Dec. 2022, Release 19.

[12] H. Godrich, A. P. Petropulu, and H. V. Poor, "Power allocation strategies for target localization in distributed multiple-radar architectures," *IEEE Trans. Signal Process.*, vol. 59, no. 7, pp. 3226–3240, Jul. 2011.

[13] T. Wang, A. Conti, and M. Z. Win, "Network navigation with scheduling: Distributed algorithms," *IEEE/ACM Trans. Netw.*, vol. 27, no. 4, pp. 1319–1329, Aug. 2019.

[14] J. J. Khalife and Z. M. Kassas, "Optimal sensor placement for dilution of precision minimization via quadratically constrained fractional programming," *IEEE Trans. Aerosp. Electron. Syst.*, vol. 55, no. 4, pp. 2086–2096, Aug. 2019.

[15] J. Lee and H. Moon, "Optimum energy allocation for a random access packet with message bits," *IEEE Trans. Veh. Technol.*, vol. 68, no. 12, pp. 12 387–12 391, Dec. 2019.

[16] G. Bartoli and D. Marabissi, "CQI prediction through recurrent neural network for UAV control information exchange under URLLC regime," *IEEE Trans. Veh. Technol.*, vol. 71, no. 5, pp. 5101–5110, May 2022.

[17] E. Maşazade, R. Niu, P. K. Varshney, and M. Keskinoz, "Energy aware iterative source localization for wireless sensor networks," *IEEE Trans. Signal Process.*, vol. 58, no. 9, pp. 4824–4835, Jun. 2010.

[18] W. W.-L. Li, Y. Shen, Y. J. Zhang, and M. Z. Win, "Robust power allocation for energy-efficient location-aware networks," *IEEE/ACM Trans. Netw.*, vol. 21, no. 6, pp. 1918–1930, Dec. 2013.

[19] Y. C. Eldar, A. Goldsmith, D. Gündüz, and H. V. Poor, *Machine Learning and Wireless Communications*. New York, NY: Cambridge University Press, 2022.

[20] X. Lin, "An overview of 5G Advanced evolution in 3GPP Release 18," *IEEE Commun. Stand. Mag.*, vol. 6, no. 3, pp. 77–83, Sep. 2022.

[21] I. Goodfellow, Y. Bengio, and A. Courville, *Deep Learning*. Cambridge, MA: MIT Press, 2017. [Online]. Available: http://www.deeplearningbook.org

[22] M. Z. Win, Y. Shen, and W. Dai, "A theoretical foundation of network localization and navigation," *Proc. IEEE*, vol. 106, no. 7, pp. 1136–1165, Jul. 2018.

[23] *Technical Specification Group Radio Access Network; Study on channel model for frequencies from 0.5 to 100 GHz*, 3rd Generation Partnership Project 3GPP™ 3GPP TR 38.901 V16.1.0 (2019-12), Dec. 2019, Release 16.

[24] A. F. Molisch *et al.*, "A comprehensive standardized model for ultrawideband propagation channels," *IEEE Trans. Antennas Propag.*, vol. 54, no. 11, pp. 3151–3166, Nov. 2006.

[25] A. Conti, M. Guerra, D. Dardari, N. Decarli, and M. Z. Win, "Network experimentation for cooperative localization," *IEEE J. Sel. Areas Commun.*, vol. 30, no. 2, pp. 467–475, Feb. 2012.

[26] S. Boyd and L. Vandenberghe, *Convex Optimization*. Cambridge, UK: Cambridge University Press, 2004.

[27] N. Shlezinger, Y. C. Eldar, and S. P. Boyd, "Model-based deep learning: On the intersection of deep learning and optimization," *IEEE Access*, vol. 10, pp. 115 384–115 398, 2022.

[28] M. Z. Win and R. A. Scholtz, "Impulse radio: How it works," *IEEE Commun. Lett.*, vol. 2, no. 2, pp. 36–38, Feb. 1998.

[29] "IEEE standard for information technology - telecommunications and information exchange between systems - local and metropolitan area networks - specific requirement part 15.4: Wireless medium access control (MAC) and physical layer (PHY) specifications for low-rate wireless personal area networks (WPANs)," *IEEE Std 802.15.4a-2007 (Amendment to IEEE Std 802.15.4-2006)*, pp. 1–203, 2007.

[30] F. Ademaj, S. Schwarz, T. Berisha, and M. Rupp, "A spatial consistency model for geometry-based stochastic channels," *IEEE Access*, vol. 7, pp. 183 414–183 427, 2019.

[31] C. A. Gómez-Vega, F. Morselli, M. Z. Win, and A. Conti, "A statistical range information model with application to UWB localization," in *Proc. Military Commun. Conf.*, San Diego, CA, Nov. 2021, pp. 538–543.

[32] M. Grant and S. Boyd, "CVX: Matlab software for disciplined convex programming, version 2.2," http://cvxr.com/cvx, Jan. 2020.